COMPUTER-CONTROLLED RS-105 TEST SYSTEM FOR 1-M EUTS

M. B. Lara, J. R. Mayes, C. Nunnally, W. C. Nunnally, J. M. Byman, D. Kohlenberg

Applied Physical Electronics L.C.,
Spicewood TX, USA

Abstract

Test procedure RS-105, within MIL-STD-461F, prescribes the use of a transverse electromagnetic (TEM) cell, or parallel plate transmission line to test equipment and subsystem enclosures against a non-classified form of the E1 nuclear electromagnetic pulse (NEMP) waveform [2]. A system is described which is capable of exposing a 1-meter cubed piece of equipment under test (EUT) to the 50 kV/m double-exponential waveform outlined in the standard. A Marx generator and peaking circuit are used to drive a TEM structure which has been optimized for performance in the metrics of waveform fidelity, mechanical strength, and reduced cost. The computer control, data acquisition, and reporting system are also discussed.

I. INTRODUCTION

Sensor and Simulations Note 402 [1] has become the basis for many of the vertical HEMP simulators in use today. The document provides a detailed analysis of the criteria used to design and fabricate a simulator of nearly any practical size. Note 402 further states that while parallel-plate transmission-line structures were used in the past, they face bandwidth limitations in comparison to the conical TEM line described in the document [1]. That being said, the parallel plate design provides several practical benefits over the conical line, and was therefore analyzed in simulation during the preliminary design phase of a simulator for use with 1-meter EUTs. These benefits are listed below:

- Easily defined, and potentially homogenous test volume.
- Closer adherence to MIL-STD-461F.
- Ability to use a lumped load instead of a resistive curtain (lower cost).

While the simulations did show that the parallel-plate design should be capable of generating the desired electric-field characteristics for the 1-meter cubed EUT structure, experimental verification seemed to corroborate the issues outlined in Note 402. Through a combination of simulation-based analysis, and experimental verification, a hybrid parallel-plate/conical-TEM structure was implemented that provided some of the benefits of the parallel plate line with the waveform fidelity delivered by the conical line.

II. FIRST-PASS SIMULATION RESULTS

MIL-STD-461F [2] was used to define an input waveform, test-volume dimensions, and acceptable test-volume waveforms for a CST simulation. A synopsis of these requirements is outlined in Table 1.

Table 1. Minimum design requirements from MIL-STD-461F

Requirement	Value	Unit	Notes
Peak Electric-Field	*50*	*kv/m*	*0 dB ≤ magnitude ≤ 6 dB*
Rise-time	*2.3*	*ns*	*+/- 5 ns*
Pulse-width	*25*	*ns*	*+/- 5 ns*
Test-volume minimum length	*2*	*m*	2A, where A is the EUT length
Test-volume minimum width	*2*	*m*	2B, where B is the EUT width
Test volume minimum height	*3*	*m*	3h, where h is the EUT height

Although, the minimum requirement for the structure width is only 2 meters, a top-plate width of 5 meters was chosen to yield a structure impedance closer to 100 ohms.

Using the above criteria as a starting point for the CST simulation, a parametric analysis was performed for feed angles of 14, 18, 22, 26 and 30 degrees. As expected, the high-frequency content of the pulse was radiated before reaching the test volume for the 22-30 degree cases, yet the 14 and 18 degree cases yielded waveforms that fell within the specification. As a result, 18 degrees was used as the feed angle for the first-pass simulator design. The simulation structure and results of the simulation are shown in Fig. 1 and Fig. 2.

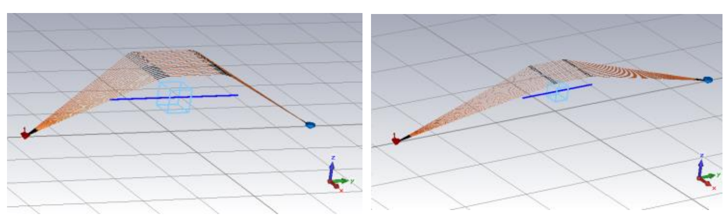

Figure 1. Parallel plate simulation structure for 30 and 14 degree feed angles

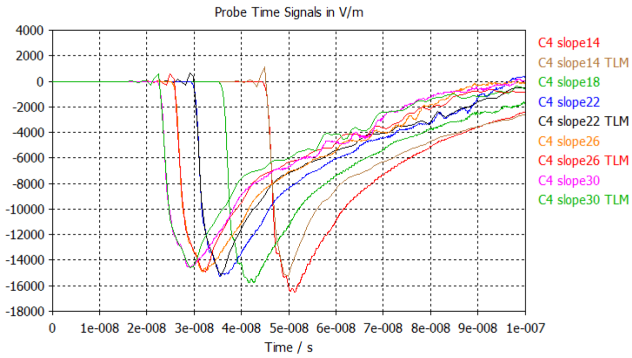

Figure 2. Simulation data for 14, 18,22,26, and 30 degree feed angles

III. Prototype Testing

A prototype of the Marx generator and peaking system was tested to ensure that the rise-time and pulse-width would be realizable with a coaxial Marx generator coupled to a planar peaking circuit. The system was fired into a resistive load, and a Prodyn AD-55 field probe was used to measure the near-field radiation from the device. The initial data was limited by the short transition section, but suggested that a rise-time on the order of 1 ns was possible. Fig. 3 shows the resultant waveform from this experiment. It can be seen that the rising edge of the pulse was interrupted by the reflection occurring where the transition section meets the load.

Figure 3. Pulsed power prototype hardware

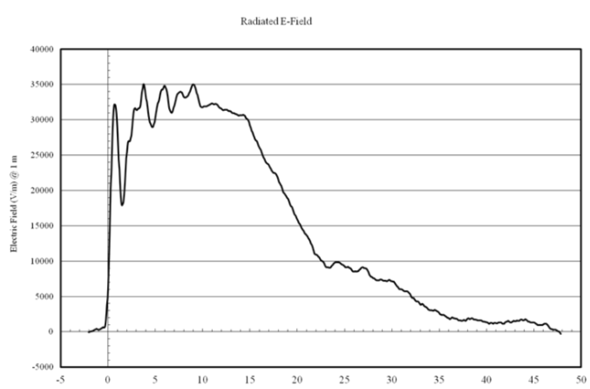

Figure 4. Pulsed power prototype waveform (dummy load)

The prototype pulse generator was then attached to a full-scale prototype radiating structure, pictured in Fig. 5. Measurements were also made using the AD-55, this time placed in the center of the test volume. The resultant waveform, shown in Fig.6, suggested that the multiple transitions within the parallel plate structure resulted in undesirable perturbations in the waveform. Consequently, a conical line was tested with a lumped load, and then modified into the final hybrid design. The results from this case are discussed in the following section.

Figure 5. Parallel-plate prototype structure

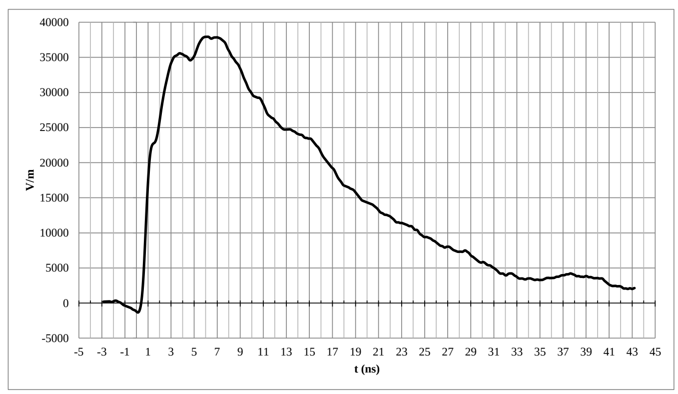

Figure 6. Parallel-plate prototype test volume waveform

IV. Hybrid TEM-line Final Design

A. *Hybrid TEM-line*

Further testing revealed that a simple conical TEM-line with a lumped load also resulted in a reflection emanating from the load-side transition. To ameliorate this issue, the structure was raised slightly to maintain the 3h height of the test volume, and the load taper was raised into a shape similar to a parallel-plate line. This had the effect of changing the direction of the unwanted reflection so that it was no longer incident upon the test volume. Also during this period of testing, the final pulsed-power was fabricated and tested. The finished design and resultant waveform are shown in Fig. 7 and Fig. 8.

Figure 7. Final Hybrid-structure

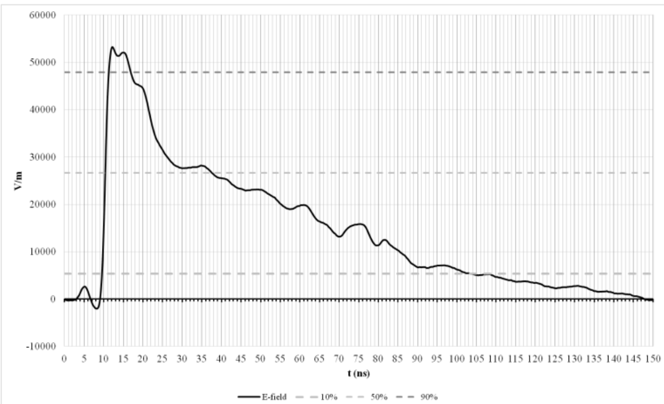

Figure 8. Final Hybrid-structure test-volume waveform

B. Pulsed Power

The pulsed-power used to drive the final design of the hybrid-TEM line consisted of a 7-stage, coaxial Marx generator driving a 40-pF, planar peaking circuit (Fig. 9). The Marx generator was contained inside of a metal pressure vessel to allow insulation of the entire Marx volume with compressed, dry, breathable air, and the peaking switch was oil-insulated. A mechanical adjustment for the peaking switch was provided on the top of the peaking container. Specifications for the pulse power are listed in Table 2.

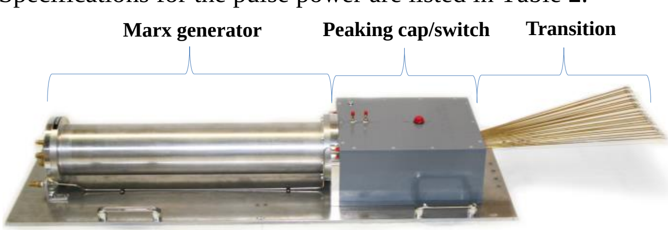

Figure 9. Coaxial Marx generator and planar peaking circuit

Table 2. Pulsed Power specifications

Specification	Value	Unit
# Marx stages	*7*	
Max charge voltage	*30*	*kV*
Max output voltage (O.C.)	*210*	*kV*
Peaking capacitance	*40*	*pF*
Peaking switch insulation	*Dry air*	
Peaking capacitor insulation	*Oil*	

V. Diagnostics

Prodyn models AD-55 and AD-110 were used for the EUT and Reference measurements respectively (Fig. 10). In accordance with the procedure outlined in MIL-STD-461F/RS105, a reference measurement was taken at the output of the pulse generator, and was simultaneously compared with the electric-field measured within the EUT volume [2]. A Microwave Photonics optical link was placed inside of a shielded enclosure, along with a battery and supporting electronics to transmit the RF signal from the probe, over fiber-optic, to the oscilloscope. Multiple experiments were performed to determine the most accurate method of transmitting and integrating the probe signal. In the end it was determined that numerical integration was preferred to passive integration for the following reasons:

- Input signal to the optical link was limited to ~300 mV.
- The passive integrator attenuated the signal by as much as 50dB, leaving the signal at the oscilloscope below the noise floor.
- Passive integrator required post-processing to correct for droop.
- While numerical integration is susceptible to noise-related errors, short, well-shielded cabling mitigated this problem.
- Offset removal built into the integration expression provided a simple method of correction.

Figure 10. Prodyn AD-55 free-field D-dot sensor (left) and Prodyn AD-110 ground-plane D-dot sensor (right)

VI. Controls

A control platform was designed and constructed that allowed for remote and local control of the high-voltage power supply and compressed dry-air insulation. A LabVIEW™ based control software was written to control the system remotely and provide automated reporting functionality. A pressure/voltage look-up table was used to automatically set charge voltage, Marx pressure, and peaking pressure based upon a set-value for desired electric-field. Communication with the local controls was conducted over fiber-optic. The remote and local control front panels are pictured in Fig. 11.

Figure 11. Remote control software (left) and local controls (right)

VII. CONCLUSIONS

An NEMP simulator was presented which was capable of testing 1-meter cubed EUT’s to MIL-STD-461F/RS-105. The simulator achieved the correct waveform using a novel coaxial Marx-generator-driven peaking switch and hybrid TEM-line design. During the design process of the simulator, it was discovered that the CST simulation used in advance of the prototype construction did not accurately predict the behavior of the radiating structure. While the parallel-plate structure was not able to generate a pulse in accordance with MIL-STD-461F, several modifications yielded a hybrid design that provided the correct waveform in the test-volume, while still offering some of the benefits of a parallel-plate structure. The final version of the simulator was constructed as a fully integrated system, which included remote software controls, reporting capabilities, and fiber-optically transmitted field/voltage probes.

VIII. REFERENCES

[1] Giri, D. V., and C. E. Baum. "Design guidelines for flat-plate conical guided-wave EMP simulators with distributed terminators." *Sensor and Simulation Notes* 402 (1996)

[2] U.S. Department of Defense. "MIL-STD-461F, Requirements for the Control of Electromagnetic Interference Characteristics of Subsystems and Equipment" (2007)